

# Spatial Risk Assessment of Rift Valley Fever in Senegal

ARCHIE C.A. CLEMENTS,<sup>1,2</sup> DIRK U. PFEIFFER,<sup>1</sup> VINCENT MARTIN,<sup>3</sup>  
CLAUDIA PITTIGLIO,<sup>3</sup> NICKY BEST,<sup>4</sup> and YAYA THIONGANE<sup>5</sup>

## ABSTRACT

Rift Valley fever (RVF) is broadening its geographic range and is increasingly becoming a disease of global importance with potentially severe consequences for human and animal health. We conducted a spatial risk assessment of RVF in Senegal using serologic data from 16,738 animals in 211 locations. Bayesian spatial regression models were developed with interpolated seasonal rainfall, land surface temperature, distance to perennial water bodies, and time of year entered as fixed-effect variables. Average total monthly rainfall during December–February was the most important spatial predictor of risk of positive RVF serologic status. Maps derived from the models highlighted the lower Senegal River basin and the southern border regions of Senegal as high-risk areas. These risk maps are suitable for use in planning improved sentinel surveillance systems in Senegal, although further data collection is required in large areas of Senegal to better define the spatial distribution of RVF.

**Key Words:** Rift Valley Fever—Bayesian methods—Geostatistics—Sentinel surveillance—Spatial prediction. Vector-Borne Zoonotic Dis. 7, 203–216.

## INTRODUCTION

RIFT VALLEY FEVER (RVF) is a mosquito-transmitted disease caused by a Phlebovirus from the *Bunyaviridae* family, affecting a wide range of mammals including domestic livestock species and man (Lefevre 1997). The main economic consequences of RVF in livestock arise due to abortion and mortality, which tends to be higher in young animals (Eisa et al. 1977, Woods et al. 2002) and the impact of animal movement and trade restrictions during an epidemic (Anyamba et al. 2001). Human infections, which are potentially fatal, usually occur during animal epidemics, in which transmission occurs either via bites from infected mosquitoes or by exposure to body fluids, tis-

sues and aborted foetuses from infected animals (Abu-Elyazeed et al. 1996, Balkhy and Memish 2003, Jouan et al. 1989, Morvan et al. 1991, Wilson et al. 1994, Woods et al. 2002).

Rift Valley fever virus (RVFV) has been isolated from a wide range of vector species in West Africa including *Aedes* sp., *Culex* sp., *Culicoides* sp., *Mansonia* sp. and *Amblyomma variegatum* (Diallo et al. 2000, Fontenille et al. 1995, 1998, Traore-Lamizana et al. 2001). The species of vectors that are capable of transmitting RVFV have a wide global distribution (Gubler 2002) and there is significant potential for spread of the virus outside its current geographic range (Brès 1981), which has continued to expand in recent decades. Epidemics of RVF have been reported throughout Africa and the

<sup>1</sup>Epidemiology Division, Department of Veterinary Clinical Sciences, Royal Veterinary College, Hatfield, Hertfordshire, United Kingdom.

<sup>2</sup>Division of Epidemiology and Social Medicine, School of Population Health, University of Queensland, Herston, Australia.

<sup>3</sup>Animal Health Service, Food and Agriculture Organisation (United Nations), Rome, Italy.

<sup>4</sup>Division of Epidemiology, Public Health and Primary Care, Imperial College, London, United Kingdom.

<sup>5</sup>Laboratoire National d'Etudes et de Recherches Vétérinaires, Institut Sénégalaïs de Recherches Agricoles (LNERV-ISRA), Dakar-Hann, Senegal.

Arabian Peninsula, including the Senegal River basin, where epidemics occurred during 1987 and 1993–1995 (Thiongane et al. 1991, Thonnon et al. 1999).

Advances in geographical information systems (GIS) and remote sensing (RS) technology have led to attempts to predict RVF epidemics using climatic indicators, with the aim of permitting early initiation of control measures, such as animal vaccination campaigns and eradication of mosquito breeding sites. Spatiotemporal analyses of normalised difference vegetation index (NDVI) data or derivations such as NDVI anomalies have been advocated for determining the timing and location of RVF epidemics in East Africa (Anyamba et al. 2001, 2002, Linthicum et al. 1987, 1999). In addition, the Southern Oscillation Index and sea surface temperatures in the Pacific and Indian Oceans (which measure the El Niño southern oscillation climatic phenomenon) have been explored as possible indicators of impending RVF epidemics in East Africa (Anyamba et al. 2001, Linthicum et al. 1999) and mapping of accumulated water (dambos) using remote sensing has been advocated to facilitate preventive action (Pope et al. 1992, Linthicum et al. 1991).

These studies have investigated the spatiotemporal distribution of RVF with the aim of predicting the timing and locations of RVF epidemics, based on existing knowledge of the ecology of RVF. However, there have been few reports where extensive epidemiologic data (e.g., serologic data) have been used to develop or validate maps of RVF distribution. In the current study, epidemiologic and ecologic information were integrated in the context of a multivariable spatial risk assessment of RVF in Senegal and surrounding countries. The aim was not to predict epidemics spatiotemporally, but to better define the spatial processes involved in disease risk, particularly to define ecological areas that are potential endemic foci of RVF and from which future epidemics may arise. Practical goals were to make recommendations for the allocation of resources to further data collection, including better positioning of sentinel surveillance sites and potential disease interventions, such as the strategic use of vaccines.

## MATERIALS AND METHODS

### *Epidemiologic data*

Serologic data for RVF were collated by staff at the Laboratoire National d'Elevage et de Recherches Vétérinaires, Institut Sénégalaïs de Recherches Agricoles and the Food and Agriculture Organisation from two separate sources: (1) bovine, ovine and caprine sentinel herds located in perceived high-risk areas of the country and (2) bovine herds that were sampled randomly during the Pan African Rinderpest Campaign (PARC). In total, 16,738 animals were sampled between November 1988 and July 2000, including 9989 cattle, 4523 sheep and 2219 goats from 439 herds (239 sentinel herds and 200 PARC survey herds) located at 211 sites throughout Senegal (56 sentinel sites and 155 PARC survey sites) (Fig. 1). Serologic status was defined on the basis of the virus neutralisation test (Swanepoel et al. 1986) for all herds in the dataset. Serological prevalence was 30.4% for the PARC herds (cattle only) and 12.2%, 9.8%, and 12.2% for the sentinel herds (cattle, sheep, and goats, respectively).

### *Ecological data*

Geographical data for potential predictor variables, including livestock densities, derived by the Environmental Research Group, Oxford, UK ([www.ergodd.zoo.ox.ac.uk/agaa/gdat/index.htm](http://www.ergodd.zoo.ox.ac.uk/agaa/gdat/index.htm)), land-cover, obtained from the University of Maryland ([www.geog.umd.edu/landcover/global-cover.html](http://www.geog.umd.edu/landcover/global-cover.html)), NDVI and satellite-derived mean land surface temperature (LST) for 1982–1998, obtained from the National Oceanographic and Atmospheric Administration's (NOAA) Advanced Very High Radiometer (AVHRR) and derived by the Department of Zoology, Oxford University (Hay et al. 2006), perennial and nonperennial water-body locations, obtained from the United States National Imagery and Mapping Agency ([www.nima.mil](http://www.nima.mil)) and processed by the Food and Agriculture Organization and elevation, obtained from an interpolated digital elevation model from the Global and Information System (GLIS) of the United States Geological Survey ([www.edc.usgs.gov/products/](http://www.edc.usgs.gov/products/)

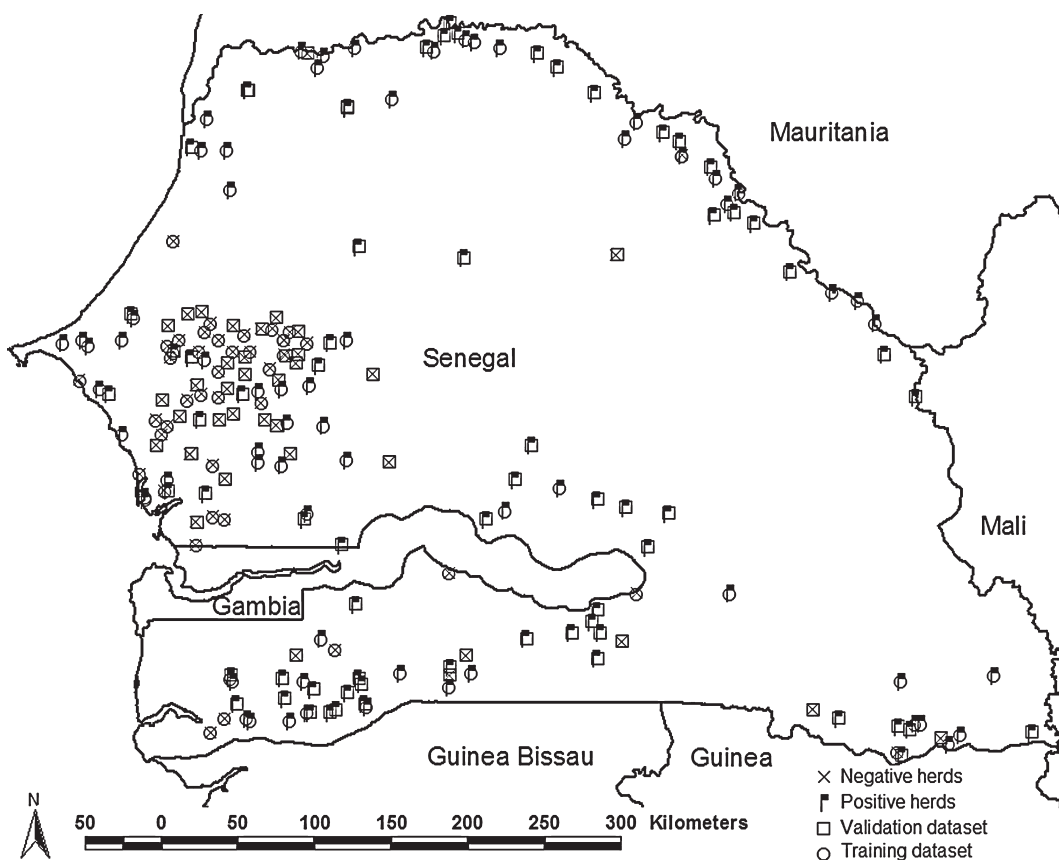


**FIG. 1.** Locations of herds in Senegal for which Rift Valley fever (RVF) serologic data were available, including the status of each location (i.e., whether or not animals were found that were serologically positive to RVF) and the analytical subset to which the data were allocated (i.e., the training subset and the validation subset).

elevation/gtopo30/gtopo30.html), were obtained. Monthly rainfall data for the years 1987–1996 were extracted from the FAOCLIM database (FAO, Rome, Italy) for Senegal and surrounding countries and the data were aggregated by season (December–February, March–May, June–August, and September–November). The driest of our season categories in Senegal was December–February followed by March–May and the wettest were June–August and September–November. Ten-year average monthly rainfall surfaces were created for each of the four seasons using geostatistical interpolation (Kriging) methods, implemented with the geostatistical analyst extension of the geographical information system (GIS) ArcMap version 8.1 (ESRI, Redlands, CA), with detrending for large-scale spatial trends and elevation. The interpolated rainfall surface for December–February (Fig. 2), unlike other seasons, was higher in northern Senegal and

southern Mauritania than in central and eastern Senegal. This is because rainfall greater than 1 mm was consistently recorded at weather stations located in the lower Senegal River basin and southern Mauritania from December–February in the years 1988–1996, but no significant rainfall was recorded in central and eastern Senegal during the same period. For the interpolation of this variable, a Gaussian model was fit to the variogram, with a nugget of 0.81, a partial sill of 4.53, and a range of 7.94 decimal degrees (approximately 970 km). For the other three seasons, a north–south gradient was apparent, with lower rainfall recorded in the north of the study area and higher rainfall recorded in the south.

#### Variable selection

Values for each of the ecological variables mentioned above were determined for all 211

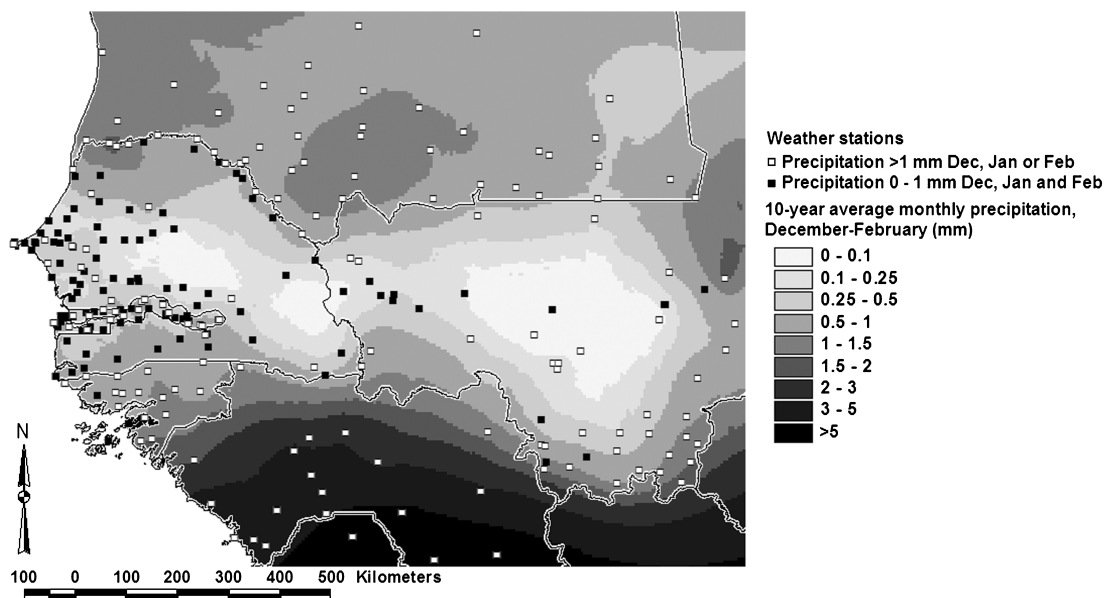


**FIG. 2.** Interpolated 10-year monthly average rainfall surface for December–February in Senegal and surrounding countries and the location of weather stations from which the data were obtained.

survey locations using ArcMap version 8.1. In addition to the ecological variables for which spatial data were available, other non-spatial variables were considered, including species present at each sampled location (cattle or mixed cattle/small ruminant), time of year during which the samples were taken (September–February, March–August and multiple seasons) and years during which the samples were taken, the latter grouped according to the amount of available data to give approximately evenly sized groups: 1988–1991, 1992–1994, and 1995–2000.

Data from each location were randomly allocated to one of two subsets: a training dataset (106 locations) and a validation dataset (105 locations) (Fig. 1). Initially, univariable logistic regression was conducted in Stata/SE version 8.0 (Stata Corporation, College Station, TX) using the training dataset. Continuous variables that were found to have a significant relationship with serologic status were then assessed for collinearity by determining the correlation between each pair of continuous variables. If unacceptable collinearity was found (correlation coefficient  $>|0.9|$ ), the variable that performed less well in predicting RVF risk at the univariable stage was excluded. The remaining

variables were then incorporated into a multi-variable logistic regression model using a backwards stepwise method of variable selection. The final model included the following predictor variables as fixed-effects: time of year, rainfall during December–February, distance to the nearest perennial water body and average LST (the first as a categorical variable and the last three as continuous variables).

#### *Bayesian model construction and selection*

Bayesian methods, which offer a flexible and robust statistical approach, are increasingly being applied to spatial analysis, disease mapping, and decision making (Best et al. 2005). They provide convenient platforms for incorporating spatial correlation and full Bayesian inference allows examination of the posterior distributions of model parameters, facilitating comprehensive assessment of uncertainty in model estimates. Logistic regression was undertaken in a Bayesian framework using the software WinBUGS version 1.4.1 (MRC Biostatistics Unit, Cambridge, UK). The training dataset was used for the analysis, with the proportion of animals testing positive at each location as the response variable and the selected

predictor variables included as fixed-effects, but without explicitly considering the spatial dependence structure of the data. Noninformative priors were specified for the intercept (uniform prior with bounds  $-\infty$  and  $\infty$ ) and the coefficients (normal priors with mean = 0 and precision =  $1 \times 10^{-6}$ ).

Spatially explicit logistic regression models were then constructed using WinBUGS version 1.4.1, with the fixed-effects described above and the spatial structure of the residuals modeled using a geostatistical design (Diggle et al. 1998). In the spatial models, the residual spatial component  $\theta_i$  was modeled using a powered exponential function:

$$f(d_{ij};\phi,\kappa) = \exp[-(\phi d_{ij})^\kappa]$$

where  $d_{ij}$  are the separating distances between pairs of points  $i$  and  $j$ ,  $\phi$  is the rate of decline of spatial correlation over distance and  $\kappa$ , set to have a value of 1, is the degree of spatial smoothing (Thomas et al. 2004). The prior distribution of  $\phi$  was a uniform distribution with the bounds set according to an examination of the observed data. A lower bound of 0.1 was specified (giving a maximum correlation of 0.25 at the maximum distance between points) to improve identifiability (Thomas et al. 2004) and an upper bound of 50 was specified to allow for rapid decay of spatial correlation. The spatial models were also run without the fixed-effects.

Three chains were run for each model and, after an initial burn-in, tests for convergence and autocorrelation were conducted. Once convergence was achieved, 10,000 values were stored for each of the model parameters and descriptive statistics were calculated for the posterior distributions of each parameter. The deviance information criterion (DIC) statistic was calculated for each of the models to determine if adding the geostatistical component and/or ecological predictors improved model fit while maintaining parsimony, as indicated by a lower value for the DIC statistic.

#### *Model validation*

Predicted risk was calculated for each location in the validation subset for the three

Bayesian models (nonspatial, spatial without covariates and spatial with covariates). For the spatial models, this involved applying the "spatial.unipred" function of WinBUGS (Thomas et al. 2004), which calculates the spatial residual component at each prediction location.

Receiver operating characteristics (ROC) analysis is being increasingly used to examine the predictive performance of spatial models (Brooker et al. 2002), where predicted risk is compared to observed risk from a validation dataset. We wanted to investigate the predictive performance of our model across a range of values of observed risk but were constrained by having sufficient positive and negative locations to allow comparison for a given gold standard threshold. This led us to choose the following two thresholds: > 0.0 (indicating presence/absence) and  $\geq 0.10$  (indicating high versus low risk). Higher prevalence thresholds were not investigated due to low numbers of high-prevalence herds in the validation subset.

The statistic used for the comparison was the area under the curve (AUC), which relates to the ROC curve, a plot of sensitivity versus one minus specificity. Values of AUC greater than 0.9 indicate an extremely well-fitting model, values greater than 0.7 indicate a moderately well-fitting model and values of 0.5 or below indicate a model that is no improvement on random allocation of test status (Brooker et al. 2002).

Additionally, the optimal prediction threshold for each model at each cutoff was calculated using two-graph ROC analysis and the sensitivity, specificity, positive predictive value (PPV) and negative predictive value (NPV) for each combination was determined at the optimal threshold, in order to understand the applicability of the models better. Fitted values of predicted risk for the training subset were also compared to observed risk using ROC analysis to gain further evidence for the goodness-of-fit of the models.

#### *Spatial predictions*

Spatial predictions were conducted at selected nonsampled locations. A grid with cell

dimensions = 0.1 decimal degrees<sup>2</sup>, calculated to give a meaningful prediction density while working within computational limitations, was overlaid on the study area. Values of the ecological variables were then determined for the prediction locations (the nodes of the grid), using ArcMap version 8.1. To allow for adjustment for season, separate prediction datasets were constructed for September–February and March–August. The model structure which gave the lowest DIC statistic was applied to the training dataset and the “spatial.unipred” function was then used to make spatial predictions at each of the prediction locations, adjusting for covariates according to each of the prediction datasets. A total of 10,000 values were stored for predicted risk and  $\theta_i$  (the spatially-structured residual) at each prediction location. Finally, maps of the summary statistics of the posterior distributions of predicted risk and  $\theta_i$  were created using ArcMap version 8.1.

## RESULTS

### The models

The Bayesian nonspatial and spatial models are presented in Table 1. The values of the DIC statistic for the nonspatial model, the spatial model without covariates, and the spatial model with covariates were 490, 360, and 347, respectively, suggesting that addition of the spatial component and the predictor variables provided a better-fitting yet parsimonious model. All covariates were significant in the Bayesian nonspatial model using the criterion of an odds ratio with 95% Bayesian credible intervals that excluded one, suggesting that risk was higher during March–August compared to September–February, risk decreased with greater distances from perennial water bodies, risk was higher in areas with higher rainfall during December–February and risk was lower in areas with higher average LST. In the model with the spatial random-effect, distance to

TABLE 1. THE BAYESIAN MODELS FOR RIFT VALLEY FEVER RISK IN SENEGL

Model/variable	Coefficients		Odds ratios	
	Posterior median	Posterior 95% Bayesian credible intervals	Posterior median	Posterior 95% Bayesian credible intervals
Nonspatial Bayesian model <sup>a</sup>				
$\alpha$ (intercept)	-2.6	-4.6–-0.5	—	—
Month of survey: March–August	1.2	0.8–1.6	3.3	2.2–5.1
Month of survey: Multiple	0.8	0.4–1.2	2.2	1.4–3.4
Distance to perennial water body	-0.8	-1.5–-0.2	0.4	0.2–0.8
Rainfall: December–February	1.7	1.4–2.0	5.6	4.2–7.5
Average land surface temperature	-0.04	-0.09–-0.002	0.96	0.91–0.998
DIC	490	—	—	—
Bayesian geostatistical model, no covariates:				
$\alpha$ (intercept)	-3.4	-3.9–-2.9	—	—
$\phi$ (correlation decay parameter)	6.0	2.4–33.6	—	—
DIC	360	—	—	—
Bayesian geostatistical model with covariates:				
$\alpha$ (intercept)	-4.9	-5.9–-4.2	—	—
Month of survey: March–August	1.9	1.1–2.9	6.8	3.0–17.6
Month of survey: Multiple	1.0	0.2–2.0	2.9	1.2–7.5
Distance to perennial water body	-0.9	-2.3–0.5	0.4	0.1–1.6
Rainfall: December–February	2.5	1.6–3.5	12.3	4.8–33.2
Average land surface temperature	0.02	-0.07–0.12	1.02	0.93–1.13
$\phi$ (correlation decay parameter)	28.5	8.8–48.9	—	—
DIC	347	—	—	—

<sup>a</sup>Note: posterior median coefficients/odds ratios were identical to the final non-spatial frequentist model.

The unit for distance to perennial water body is decimal degrees, for rainfall December–February it is millimeters and for average land surface temperature it is degrees Celsius. The reference category for month of survey is September–February (odds ratio = 1).

perennial water body and average LST were no longer significant and the coefficients were similar to those in the nonspatial model for all covariates except average LST, which had a positive (although not significant) association with risk after accounting for spatial correlation.

The rate of decay of spatial correlation in the Bayesian spatial models with and without covariates is presented in Figure 3. The range of spatial correlation, where the value decreased to less than 0.05, was approximately 0.5 decimal degrees for the model without covariates but was approximately 0.1 decimal degrees for the model that included covariates (Note: 1 decimal degree equates approximately to 122 km at the equator).

The validation statistics for predictions based on the three models are presented in Table 2. Values of 0.76–0.82 for the AUC suggested that all of the models performed well in predicting risk at the validation locations. In support of the DIC statistics, the spatial models provided a much better fit to the observed data in the training dataset when compared to the non-spatial model. However, the three models had a similar predictive performance at the validation locations.

Using the observed risk cutoff of 0.10, the optimal prediction threshold was lower overall than the equivalent observed data cutoff suggesting that, for practical application of the

maps, a value lower than 0.10 should be selected to indicate areas with true values above and below this threshold. In the case of the Bayesian geostatistical model with covariates, a predicted value of 0.038 should be used to delineate areas with true risk above and below 10%. With the same model, a predicted value of 0.025 should be used to delineate areas where RVF is likely to be absent from those where RVF is likely to be present. At these thresholds, moderately good values of sensitivity, specificity, PPV, and NPV were achieved.

#### Rift Valley fever risk predictions

All maps of predicted risk were based on the Bayesian spatial model with covariates. Maps of the posterior median predicted risk for March–August and September–February are presented in Figures 4 and 5. The maps show foci of high risk in the lower Senegal River basin, Southern Mauritania, and the border regions between Senegal and Guinea and Guinea Bissau. The areas of lowest predicted risk were in central and eastern Senegal. The maps demonstrate a constant, overall higher risk in March–August compared to September–February, although the models used (which are not explicitly spatiotemporal) did not allow the spatial pattern to vary for the different time periods.

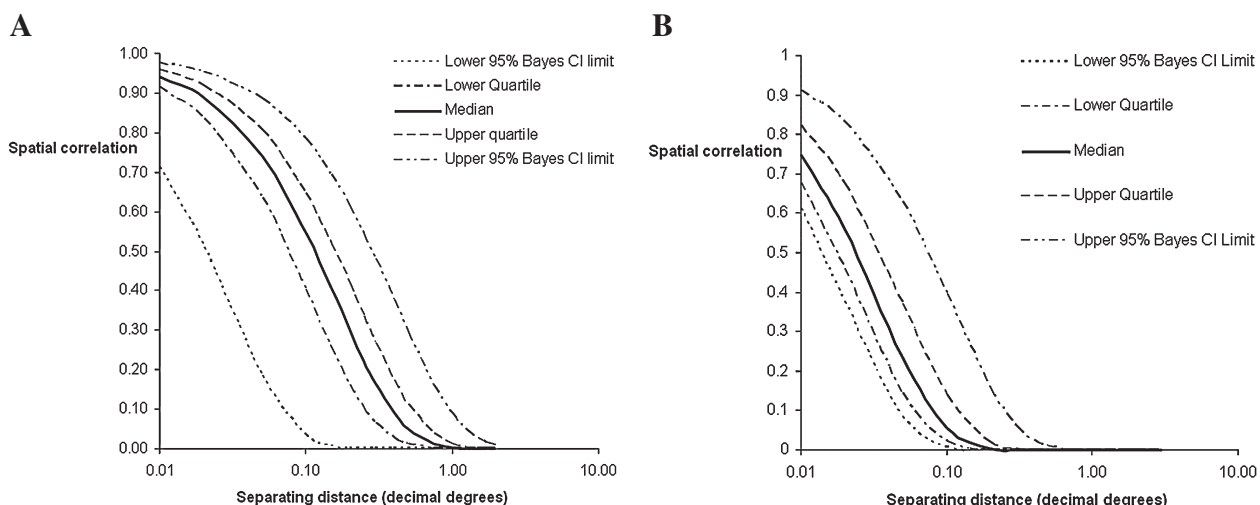


**FIG. 3.** Decay of spatial correlation of Rift Valley fever in Senegal in (A) the Bayesian geostatistical model without covariates and (B) the Bayesian geostatistical model with covariates.

TABLE 2. RESULTS OF THE RECEIVER OPERATING CHARACTERISTICS (ROC) ANALYSIS, COMPARING PREDICTED RISK FOR THE VALIDATION AND TRAINING DATASETS TO THE OBSERVED RISK USING THREE GOLD STANDARD (GS) THRESHOLDS (0.00, 0.05, 0.10), FOR EACH OF THE RIFT VALLEY FEVER REGRESSION MODELS

Model/GS threshold	AUC	Optimal prediction threshold	Se (%)	Sp (%)	PPV (%)	NPV (%)
A. Validation dataset						
Bayesian nonspatial model:						
0.00	0.82	0.040	76.1	71.1	82.3	62.8
0.05	0.78	0.047	69.6	66.1	61.5	73.6
0.10	0.80	0.058	71.4	70.1	46.5	87.1
Bayesian geostatistical model, no covariates:						
0.00	0.76	0.028	79.7	56.5	70.2	68.4
0.05	0.81	0.028	66.1	84.8	84.8	66.1
0.10	0.80	0.033	52.6	88.1	71.4	76.6
Bayesian geostatistical model with covariates:						
0.00	0.82	0.025	76.1	68.4	81.0	61.9
0.05	0.78	0.034	65.2	72.9	65.2	72.9
0.10	0.76	0.038	64.3	68.8	42.9	84.1
B. Training dataset						
Bayesian nonspatial model:						
0.00	0.82	0.038	76.9	70.7	80.7	65.9
0.05	0.84	0.045	76.2	70.3	62.8	81.8
0.10	0.81	0.053	73.7	74.7	38.9	92.9
Bayesian geostatistical model, no covariates:						
0.00	0.98	0.018	93.8	88.1	92.3	90.2
0.05	0.99	0.038	95.0	93.9	90.5	96.9
0.10	0.99	0.078	85.7	98.8	94.7	96.6
Bayesian geostatistical model with covariates:						
0.00	0.96	0.022	81.5	90.2	93.0	75.5
0.05	0.99	0.036	97.6	95.3	93.2	98.4
0.10	0.99	0.077	94.7	94.3	78.3	98.8

Apart from the area under the curve (AUC), test statistics were measured at the optimal threshold of the predicted values for differentiating observed status with sensitivity; Sp, specificity; PPV, positive predictive value; NPV, negative predictive value.

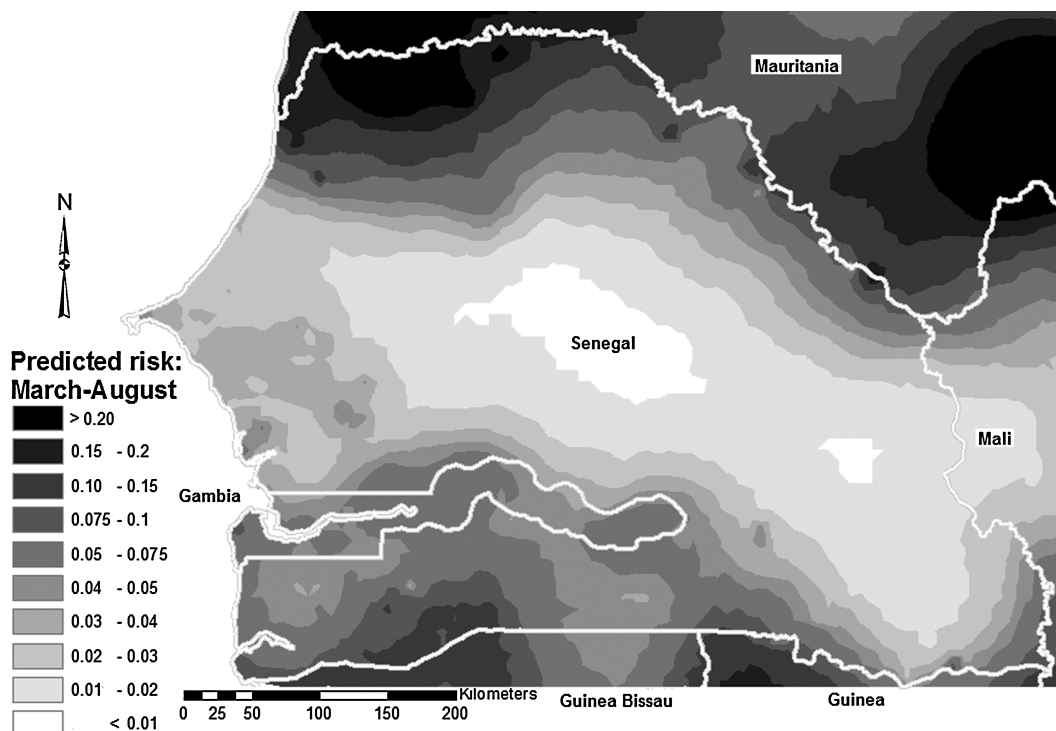
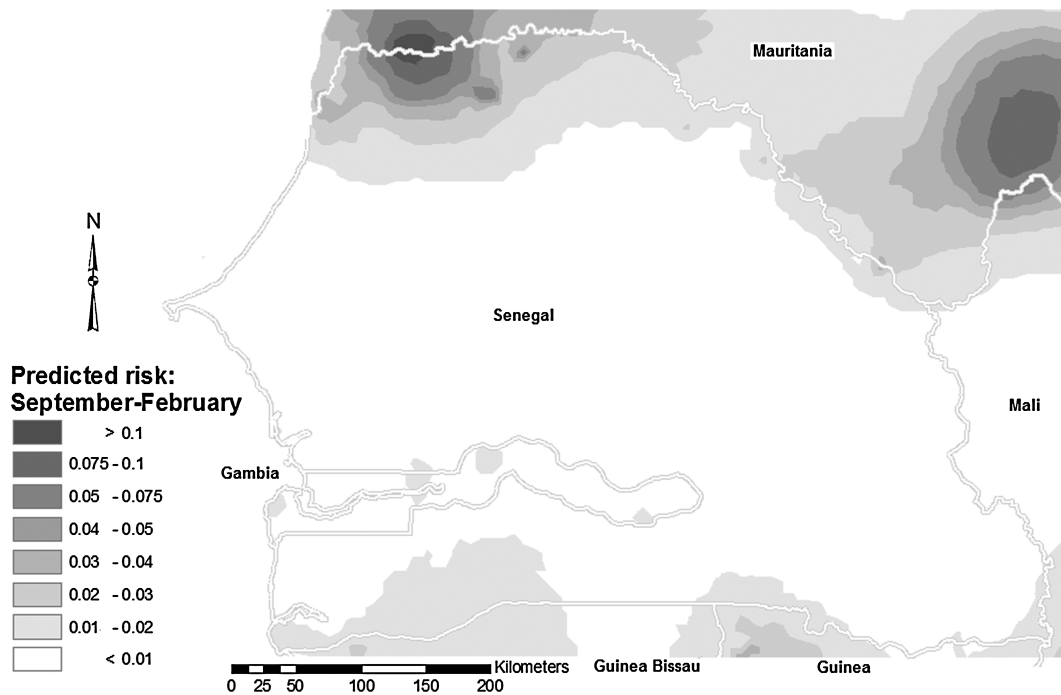


FIG. 4. Median predicted risk for Rift Valley fever in Senegal and surrounding areas based on the Bayesian geostatistical model with covariates, March–August.



**FIG. 5.** Median predicted risk for Rift Valley fever in Senegal and surrounding areas based on the Bayesian geostatistical model with covariates, September–February.

Maps of the standard deviation of posterior predicted risk for the two time periods (Fig. 6 and 7) show higher standard deviations in areas with higher predicted risk. A map of the

geostatistical component (Fig. 8) shows that most of the study area had a value close to zero (the overall mean of the spatial component), with small areas (those close to observed data

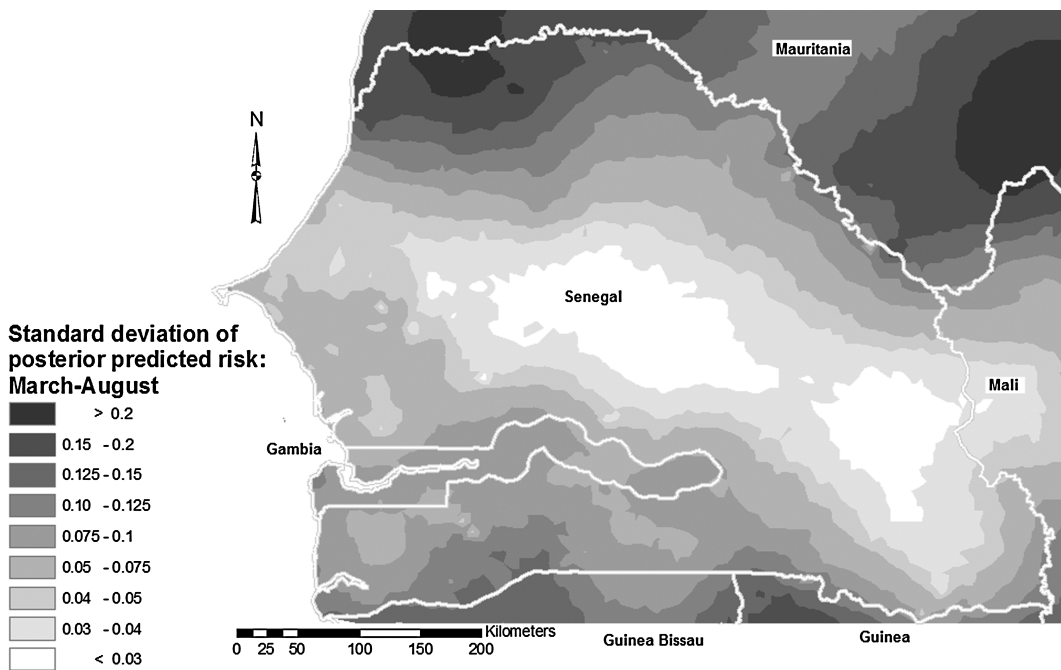


**FIG. 6.** Standard deviation of posterior predicted risk for Rift Valley fever in Senegal and surrounding areas based on the Bayesian geostatistical model with covariates, March–August.

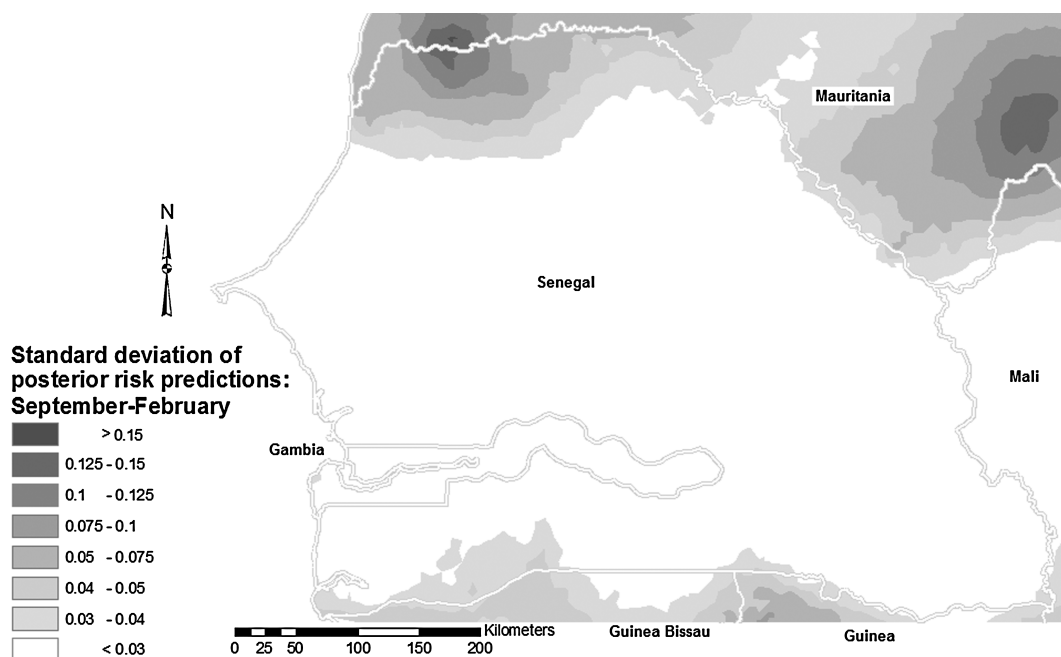


**FIG. 7.** Standard deviation of posterior predicted risk for Rift Valley fever in Senegal and surrounding areas based on the Bayesian geostatistical model with covariates, September–February.

locations) having significant positive or negative values. This reflected the small range of spatial correlation once the covariates were included in the spatial model. Therefore, predic-

tions close to observed data locations were based on the covariates plus the spatial random-effect but predictions in all other locations were only based on the covariates. Significant

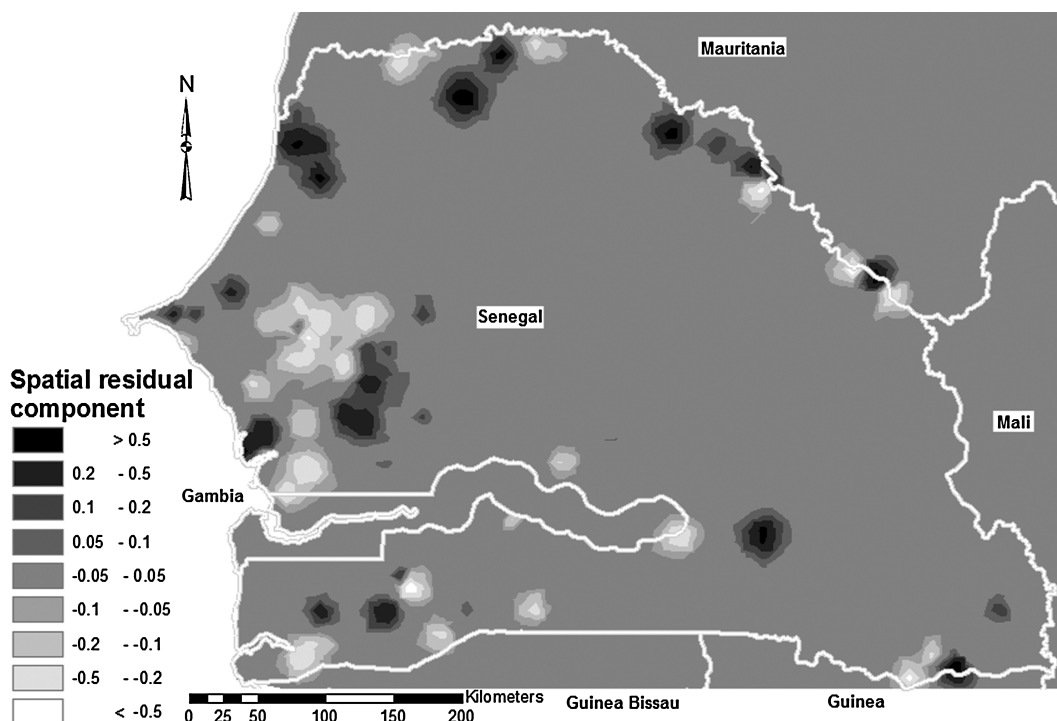


**FIG. 8.** The spatial residual component of the Bayesian geostatistical model with covariates for Rift Valley fever in Senegal and surrounding areas.

positive and negative values for the spatial random-effect were scattered in all areas where data were collected, although areas adjacent to the Senegal River had predominantly positive values and areas in central Senegal had predominantly negative values, suggesting that other spatial factors, in addition to those included in the model, were important determinants of small-scale spatial variation in RVF risk.

## DISCUSSION

Much of the previous work in RVF epidemiology has concentrated on epidemics and less is known about the endemic cycle. Climatic conditions, particularly the amount, timing and duration of rainfall have been demonstrated to be strongly associated with the precipitation of a number of RVF epidemics (Anyamba et al. 2001, Davies et al. 1985, Eisa et al. 1977, Fontenille et al. 1995, 1992, Linthicum et al. 1999, Nabeth et al. 2001, Tessier et al. 1987, Thonnon et al. 1999, Wilson et al. 1994, Zeller et al. 1997), mainly reflecting the relationship between precipitation and vector population density (Bicout and Sabatier 2004). Unusually high rainfall for a given area appears to be more important than the actual amount of rain (Swanepoel 1981, Tessier et al. 1987). However, the relationship between rainfall and RVF activity is not always straightforward. For example, RVFV transmission in man and livestock was reported during a drought in Mauritania (Saluzzo et al. 1987) and during low-rainfall years in Madagascar (Morvan et al. 1991, 1992a, 1992b).

Temperature may also have an impact on the ecology of RVF, particularly as a result of its effect on the vector. As temperatures decreases, increased mosquito longevity may lead to prolonged transmission of RVFV (Arthur et al. 1993) to a point below which mosquitoes can no longer survive. Temperature also has an impact on the ability of the vector to transmit RVFV, with higher transmission occurring at higher temperatures in *Aedes* (Turrell 1989, 1993) and *Culex* (Brubaker 1998). However, temperature was not a significant predictor of risk of positive RVFV serological status in our models after accounting for spatial correlation.

Our results suggested that the main spatial predictor for RVF serologic status in Senegal was average total monthly rainfall during December–February, which was the driest period of the year in this region. Largely as a result of the spatial distribution of rainfall in December–February, we highlighted the lower Senegal River Basin and Southern Mauritania as high-risk areas for RVF, which is consistent with the location of reported epidemics (Thiongane et al. 1991, Thonnon et al. 1999). Interestingly, the southern border region of Senegal was also identified as a high-risk area. No large epidemics have been recorded in this area and this result requires further investigation, particularly as endemic transmission in southern Senegal may play a role in the occurrence of epidemics in migrating herds. One competing hypothesis for the high risk of positive serologic status in the lower Senegal River basin is that it is a signature, arising as a result of a temporal lag in the population level of protective antibodies, of sporadically occurring epidemics. However, our results suggest that both northern and southern Senegal may be ecologically suitable for the existence of endemic foci and that this suitability may be contributed to by low-level rainfall during the dry season. Because of the consistently higher rainfall recordings in the lower Senegal River basin and southern Mauritania than in central and eastern Senegal over the time during which the epidemiologic data were collected, we feel that our results are unlikely to be the consequence of a small number of aberrant high recordings or other causes of error. External validation of the rainfall data and our interpolated rainfall maps would be necessary before this hypothesis can be confirmed and this is an area for further research.

The epidemiologic situation in west Africa is complicated by the widespread seasonal movement of livestock. Animals that are serologically positive may have been exposed far from their current location when tested, making it difficult to determine associations between the epidemiological data and ecological predictors. Temporal variation adds a further dimension to the epidemiology of RVF. Temporal and spatiotemporal correlation was not explicitly incorporated in our models, partly due to the fact

that insufficient data were available. However, we did account for seasonal variation by adding time of year of data collection as a fixed-effect and for long-term temporal variation by including year of data collection, which was not significant in the multivariable models.

A major issue in the current study was that the data were derived from two surveys with different objectives and study designs, neither of which was aimed at providing optimal data for subsequent spatial analysis. The observed data were clustered in different areas of the country and some areas (e.g., much of the eastern interior of the country) had a very low sampling density.

Unsurprisingly, the spatially explicit models provided a better fit to the training dataset than the nonspatial models. However, they did not confer a considerable advantage over the non-spatial model in terms of making predictions because our data did not have sufficient sampling density to make predictions in the validation locations, given the short range of correlation in the spatial models. The range of correlation in the spatial model with covariates was less than that of the range of correlation in the spatial model without covariates, probably because the covariates explained much of the mid- and large-scale spatial variation in the data. The range of spatial correlation presented in this study can assist the planning of future surveys by informing calculations of optimal sampling grid dimensions—sampling with a higher density leads to collection of obsolete data, whereas sampling with a lower density may lead to important clusters being overlooked.

One of the outcomes of the current study is recognition that more data collection is required if we are to properly define the small-scale spatial distribution of RVF in Senegal. However, the importance of determining small-scale spatial variation for RVF control and the cost effectiveness of surveying with a high sampling density need to be taken into consideration before we would recommend undertaking such data collection. While more widespread collection of high-quality epidemiologic data using study designs that explicitly consider spatial analytical approaches would be ideal, it is currently more realistic to recom-

mend pragmatic approaches for studying spatial and spatiotemporal patterns of RVF, that represent uncertainty in the data and that are able to incorporate additional information, including expert opinion and published data. Approaches to consider include stochastic simulation modeling, Dempster-Shafer theory, and fuzzy logic. In the meantime we can feel more optimistic of our ability to predict large-scale spatial patterns using ecological predictor variables. Our risk maps based on large-scale ecological predictors will be useful to animal health decision-makers in Senegal for planning sentinel surveillance in known high-risk areas (the lower Senegal River basin), spatially targeting vaccination programs more efficiently in contiguous high-risk areas and directing more detailed epidemiologic and entomological investigations in geographical areas that we have highlighted as having high risk for RVF, such as southern Senegal. As more serologic and entomological data become available, revalidation and revision of the maps presented in this report are recommended.

## ACKNOWLEDGMENTS

Archie Clements was supported by a Royal Veterinary College Clinical Training Fellowship. We thank Baba Sall, Direction de l'Evage, Dakar, Senegal, for his work on collecting the serum samples and his contributions toward validating the serologic data.

## REFERENCES

- Abu-Elyazeed, R, El-Sharkawy, S, Olson, J, Botros, B, et al. Prevalence of anti-Rift-Valley-fever IgM antibody in abattoir workers in the Nile delta during the 1993 outbreak in Egypt. *B World Health Organ* 1996; 74:155–158.
- Anyamba, A, Linthicum, KJ, Tucker, CJ. Climate-disease connections: Rift Valley fever in Kenya. *Cad Saude Publica* 2001; 17(suppl ):133–140.
- Anyamba, A, Linthicum, KJ, Mahoney, R, Tucker, CJ, et al. Mapping potential risk of Rift Valley fever outbreaks in African savannas using vegetation index time series data. *Photogramm Eng Rem S* 2002; 68:137–145.
- Arthur, RR, El-Sharkawy, MS, Cope, SE, Botros, BA, et al. Recurrence of Rift Valley fever in Egypt. *Lancet* 1993; 342:1149–1150.

- Balkhy, HH, Memish, ZA. Rift Valley fever: an uninvited zoonosis in the Arabian peninsula. *Int J Antimicrob Ag* 2003; 21:153–157.
- Best, N, Richardson, S, Thomson, A. A comparison of Bayesian spatial models for disease mapping. *Stat Methods Med Res* 2005; 14:35–59.
- Bicout, DJ, Sabatier, P. Mapping Rift Valley fever vectors and prevalence using rainfall variations. *Vector-Borne Zoonot* 2004; 4:33–42.
- Brès, P. Prevention of the spread of Rift Valley fever from the African continent. *Contributions to Epidemiology and Biostatistics* 1981; 3:178–190.
- Brooker, S, Hay, SI, Bundy, D. Tools from ecology: useful for evaluating infection risk models? *Trends Parasitol* 2002; 18:70–74.
- Brubaker, JF, Turrel, MJ. Effect of environmental temperature on the susceptibility of *Culex pipiens* (Diptera: Culicidae) to Rift Valley fever virus. *J Med Entomol* 1998; 35:918–921.
- Davies, FG, Linthicum, KJ, James, AD. Rainfall and epizootic Rift Valley fever. *Bull World Health Organ* 1985; 63:941–943.
- Davies, FG, Kilelu, E, Linthicum, KJ, Pegram RG. Patterns of Rift Valley fever activity in Zambia. *Epidemiol Infect* 1992; 108:185–191.
- Diallo, M, Lochoourn, L, Ba, K, Sall, AA, et al. First isolation of the Rift Valley fever virus from *Culex poicilipes* (Diptera: Culicidae) in nature. *Am J Trop Med Hyg* 2000; 62:702–704.
- Diggle, PJ, Tawn, JA, Moyeed, RA. Model-based geostatistics. *Appl Stat* 1998; 47:299–350.
- Eisa, M, Obeid, HMA, El-Sawi, ASA. Rift Valley fever in the Sudan. Results on field investigations of the first epizootic in Kosti District, 1973. *Bull Anim Health Prod Afr* 1977; 25:343–347.
- Fontenille, D, Traore-Lamizana, M, Zeller, H, Mondo, M, et al. Rift Valley fever in Western Africa: isolations from Aedes mosquitoes during an interepizootic period. *Am J Trop Med Hyg* 1995; 52:403–404.
- Fontenille, D, Traore-Lamizana, M, Diallo, M, Thonnon, J, et al. New vectors of Rift Valley fever in West Africa. *Emerg Infect Dis* 1998; 4:289–293.
- Gubler, DJ. The global emergence/resurgence of arboviral diseases as public health problems. *Arch Med Res* 2002; 33:330–342.
- Hay SI, Tatem AJ, Graham AJ, Goetz SJ, Rogers DJ. Global environmental data for mapping infectious disease distribution. *Adv Parasitol* 2006; 62:37–77.
- Jouan, A, Coulibaly, I, Adam, F, Philippe, B, et al. Analytical study of a Rift Valley fever epidemic. *Res Virology* 1989; 140:175–186.
- Lefevre, PC. Actualité de la fièvre de la Vallée du Rift quels enseignements tirez des épidémies de 1977 et 1987? *Med Trop* 1997; 57:61–64.
- Linthicum, KJ, Bailey, CL, Davies, FG, Tucker, CJ. Detection of Rift Valley fever viral activity in Kenya by satellite remote sensing imagery. *Science* 1987; 235:1656–659.
- Linthicum, KJ, Bailey, CL, Tucker, CJ, Angleberger, DR, et al. Towards real-time predictions of Rift Valley fever epidemics in Africa. *Prev Vet Med* 1991; 11:325–334.
- Linthicum, KJ, Anyamba, A, Tucker, CJ, Kelley, PW, et al. Climate and satellite indicators to forecast Rift Valley fever epidemics in Kenya. *Science* 1999; 285: 397–400.
- Morvan, J, Saluzzo, JF, Fontenille, D, Rollin, PE, et al. Rift Valley fever on the east coast of Madagascar. *Res Virology* 1991; 142:475–482.
- Morvan, J, Rollin, PE, Roux, J. Situation de la fièvre de la Vallée du Rift à Madagascar en 1991. Enquêtes séro-épidémiologiques chez les bovins. *Rev Élev Med Vet Pay* 1992a; 45:121–127.
- Morvan, J, Rollin, PE, Laventure, S, Rakotoarivony, I, et al. Rift Valley fever epizootic in the central highlands of Madagascar. *Res Virology* 1992b; 143:407–415.
- Nabeth, P, Kane, Y, Abdalahi, MO, Diallo, M, et al. Rift Valley fever outbreak, Mauritania, 1998: seroepidemiologic, virologic, entomologic and zoologic investigations. *Emerg Infect Dis* 2001; 7:1052–1054.
- Pope, KO, Sheffner, EJ, Linthicum, KJ, Bailey, CL, et al. Identification of Central Kenyan Rift Valley fever virus vector habitats with Landsat TM and evaluation of their flooding status with airborne imaging radar. *Remote Sens Environ* 1992; 40:185–196.
- Saluzzo, JF, Digoutte, JP, Chartier, C, Martinez, D, et al. Focus of Rift Valley fever virus transmission in Southern Mauritania. *Lancet* 1987; 1:504.
- Swanepoel, R. Observations on Rift Valley fever in Zimbabwe. *Contrib Epidemiol Biostat* 1981; 3:83–91.
- Swanepoel R, Struthers JK, Erasmus MJ, Shepherd SP, McGillivray GM, Erasmus BJ, Barnard BJ. Comparison of techniques for demonstrating antibodies to Rift Valley fever virus. *J Hyg (Lond)* 1986; 97:317–329.
- Tessier, SF, Rollin, PE, Sureau, P. Viral haemorrhagic fever survey in Chobe (Botswana). *T Roy Soc Trop Med H* 1987; 81:699–700.
- Thiongane, Y, Gonzalez, JP, Fati, A, Akakpo, JA. Changes in Rift Valley fever neutralizing antibody prevalence among small domestic ruminants following the 1987 outbreak in the Senegal River basin. *Res Virology* 1991; 142:67–70.
- Thomas, A, Best, N, Lunn, D, Arnold, R, et al. Geobugs user manual. 2004. [www.mrc-bsu.cam.ac.uk/bugs](http://www.mrc-bsu.cam.ac.uk/bugs). (Last accessed May 11, 2007).
- Thonnon, J, Picquet, M, Thiongane, Y, Lo, M, et al. Rift Valley fever surveillance in the lower Senegal River basin: update 10 years after the epidemic. *Trop Med Int Health* 1999; 4:580–585.
- Traore-Lamizana, M, Fontenille, D, Diallo, M, Ba, Y et al. Arbovirus surveillance from 1990 to 1995 in the Barkedji area (Ferlo) of Senegal, a possible natural focus of Rift Valley fever virus. *J Med Entomol* 2001; 38:480–492.
- Turrell, MJ. Effect of environmental temperature on the vector competence of *Aedes fowleri* for Rift Valley fever virus. *Res Virology* 1989; 140:147–154.
- Turrell, MJ. Effect of environmental temperature on the vector competence of *Aedes taeniorhynchus* for Rift Val-

- ley fever and Venezuelan equine encephalitis viruses. Am J Trop Med Hyg 1993; 49:672–676.
- Wilson, ML, Chapman, LE, Hall, DB, Dykstra, EA, et al. Rift Valley fever in rural Northern Senegal: human risk factors and potential vectors. Am J Trop Med Hyg 1994; 50:663–675.
- Woods, CW, Karpati, AM, Grein, T, McCarthy, N, et al. An outbreak of Rift Valley fever in Northeastern Kenya, 1997–98. Emerg Infect Dis 2002; 8:138–144.
- Zeller, HG, Fontenille, D, Traore-Lamizana, M, Thiongane, Y, et al. Enzootic activity of Rift Valley fever virus in Senegal. Am J Trop Med Hyg 1997; 56:265–272.

Address reprint requests to:

*Dr. Archie C. A. Clements*

*Division of Epidemiology and Social Medicine*

*School of Population Health*

*University of Queensland*

*Herston Road*

*Herston*

*Queensland 4006*

*Australia*

*E-mail:* a.clements@sph.uq.edu.au